Vacancy complexes with oversized impurities in Si and Ge

H. Höhler, N. Atodiresei, K. Schroeder, R. Zeller, and P. H. Dederichs
Institut für Festkörperforschung, Forschungszentrum Jülich, D-52425 Jülich, Germany
(Received 9 July 2004; revised manuscript received 25 October 2004; published 21 January 2005)

In this paper we examine the electronic and geometrical structure of impurity-vacancy complexes in Si and Ge. Already Watkins suggested that in Si the pairing of Sn with the vacancy produces a complex with the Sn-atom at the bond center and the vacancy split into two half vacancies on the neighboring sites. Within the framework of density-functional theory we use two complementary *ab initio* methods, the pseudopotential-plane-wave method and the all-electron Kohn-Korringa-Rostoker method, to investigate the structure of vacancy complexes with 11 different *sp*-impurities. For the case of Sn in Si, we confirm the split configuration and obtain good agreement with EPR data of Watkins. In general we find that all impurities of the 5*sp* and 6*sp* series in Si and Ge prefer the split-vacancy configuration, with an energy gain of 0.5–1 eV compared to the substitutional complex. On the other hand, impurities of the 3*sp* and 4*sp* series form a (slightly distorted) substitutional complex. Al impurities show an exception from this rule, forming a split complex in Si and a strongly distorted substitutional complex in Ge. We find a strong correlation of these data with the size of the isolated impurities, being defined via the lattice relaxations of the nearest neighbors.

DOI: 10.1103/PhysRevB.71.035212 PACS number(s): 71.55.Cn, 76.60.−k, 61.72.Ji, 71.15.Mb

I. INTRODUCTION

Intrinsic defects and their complexes with impurities play an important role in semiconductor physics. In this paper we present *ab initio* calculations for vacancy-impurity complexes in Si and Ge. Based on EPR measurements, Watkins[1] has already shown that in Si the Sn-vacancy complex prefers an exotic configuration, i.e. a split-vacancy complex with the Sn atom on the bond-center position and the vacancy split into two half-vacancies on the nearest neighbor (NN) sites. This configuration has been supported by *ab initio* calculations for Sn in Si by Larsen *et al.*[2] and Kaukonen *et al.*,[3] reporting a small energy preference of 0.045 eV for this complex compared to the configuration with substitutional Sn and the vacancy on NN sites.

Recently we have studied by density functional calculations the Cd-vacancy and Cd-interstitial complexes in Si and Ge,[4] aiming at understanding the electric field gradients (EFG) measured in perturbed angular correlation (PAC) experiments for the ^{111}In/^{111}Cd probe atom. We find that both in Si and Ge the substitutional Cd-vacancy complex is instable and relaxes into the highly symmetrical Cd-split-vacancy complex, being about 1 eV lower in energy than the substitutional configuration. In the split configuration the Cd atom hybridizes very weakly with the six Si or Ge nearest neighbors, resulting in a nearly isotropic charge density and an extremely small EFG. In this way we find good agreement with PAC measurements and can uniquely assign the very small measured Cd EFG's of 28 MHz in Si and 54 MHz in Ge to the Cd-split-vacancy complex. In parallel to our calculations Alippi *et al.* show in a recent publication,[5] that in Si also In impurities form such a split configuration with the vacancy, exhibiting an unusually large binding energy of 2.4 eV.

The present paper has a twofold aim. First we present *ab initio* calculations for the electronic and geometrical structure of the Sn-vacancy complex in Si and Ge. In particular we concentrate on the hyperfine properties of this defect for the different charge states, i.e., the hyperfine fields, the isomer shifts and the electric field gradients, and compare with available experimental data by Watkins[1] and others.[6,7] These properties have not been calculated so far, since they are difficult to obtain by the standard pseudopotential-plane-wave method. In the second part of the paper the structure of impurity-vacancy complexes for other impurities is calculated, in particular for heavy impurities with larger sizes than Si or Ge atoms. For the elements Cd, In, Sn, and Sb of the 5*sp* series we find that both in Si and Ge the split-vacancy impurity complex is preferred over the substitutional one by energies between 0.5 to 1 eV, being slightly larger in Si than in Ge. The results for the even heavier element Bi of the 6*sp* series suggest, that in Si and Ge this is the stable configuration for all oversized impurities. On the other hand, the calculations show that impurities of the 3*sp* and 4*sp* series, with the exception of Al in Si, prefer the substitutional complex. In order to discuss the importance of impurity size for the relative stability of the substitutional and split configurations we calculate the lattice relaxations of the nearest neighbors for a large series of isolated impurities from the 3*sp*, 4*sp*, and 5*sp* series. In general, we find a good qualitative correlation of the sign and size of the NN relaxations with the stability of the two configurations, although a strict one-to-one correspondence is not valid.

II. THEORETICAL METHODS

All calculations are based on density functional theory in the local density approximation.[8] Two different methods have been used to solve the Kohn-Sham equations. The first one is the pseudopotential-plane-wave (PPW) method, which has mostly been used to investigate the configuration and stability of the impurity-vacancy configurations. These configurations, as well as the relaxations of the neighboring atoms, have been recalculated by the KKR-Green function

method[9,10] for the Sn-impurity, which as an all-electron method allows also to calculate electric field gradients, isomer shifts and hyperfine fields.[11,12]

The PPW method approximates the inhomogeneous systems containing defect complexes by periodically arranged large supercells, and uses plane waves to expand the electronic wave functions. This has the advantage that band-structure methods can be used to determine the electronic structure, and total energies and forces on the atoms can be calculated without difficulty for arbitrary arrangements of the atoms in the supercell. We have used norm-conserving Kleinman-Bylander (KB) pseudopotentials[13] for all atoms considered, where the s,p-valence electrons are treated by projectors, and the $d(l=2)$-component is used as a local potential. Our EStCoMPP program[14] is fully parallelized and can efficiently handle supercells with up to 300 atoms. For the calculations of impurity-vacancy complexes we used a (111)-oriented supercell with the basis vectors $\mathbf{b}_1=(3/2)a(0,-1,1);\mathbf{b}_2=(3/2)a(-1,1,0);\mathbf{b}_3=2a(1,1,1)$ containing 108 atoms. a is the theoretical lattice constant ($10.71a_B$ for Ge with $E_{\mathrm{cut}}=11.56$ Ry, and $10.25a_B$ for Si with $E_{\mathrm{cut}}=9$ Ry; Bohr radius $a_B=0.529\,177$ Å). The impurity-complexes were placed in the middle of the cell. We used C_{3v} symmetry explicitly for all configurations. The isolated substitutional impurities were calculated with a $2\times2\times2$ a^3 cubic cell containing 64 atoms. The impurities were located at the central site, and the T_d site-symmetry is enforced. A plane-wave basis set equivalent to $6\times6\times6$ Monkhorst-Pack[15] **k**-points was used which yields three inequivalent **k**-points in the irreducible part of the Brillouin-zone for the 108-atom-supercell and five inequivalent **k**-points for the 64-atom-supercell. We used a plane-wave cut-off $E_{\mathrm{cut}}=9$ Ry for impurities in Si, and $E_{\mathrm{cut}}=11.56$ Ry for impurities in Ge. The atoms belonging to the impurity-complexes and their nearest neighbors were relaxed until the forces on all atoms were less than 0.1 mRy/a_B. We checked that forces on further neighbors (which were not moved) were less than 20 mRy/a_B. The Sn-complexes in both hosts were recalculated for a cut-off energy of 13.67 Ry, and we found no significant changes of the configurations or the energy differences for the tested configurations. We estimate that the positions of all relaxed atoms are determined with an accuracy better than $0.01a_B$, and the energy differences are accurate to about 0.1 eV.

In the KKR-Green function method the calculation is divided in two steps. First the Green function of the host is determined. In a second step the host Green function is used to determine the Green function of the crystal with a single impurity by a Dyson equation. For details we refer to Ref. 16. All calculations are performed with an angular momentum cut-off of $l_{\max}=4$. For the host crystal we use the LDA lattice constants[18] of Si ($10.21a_0$) and Ge ($10.53a_0$). A k-mesh of $30\times30\times30$ **k**-points in the full Brillouin zone is used. We use the screened KKR-formalism[10,19,20] with the tight-binding structure constants determined from a cluster of 65 repulsive potentials of 4 Ry heights. The diamond structure is described by a unit cell with four basis sites, two for host atoms and two for vacant sites. For the Green function of the defective systems, we allow 77 potentials of the defect and the surrounding host atoms to be perturbed, which are then calculated self-consistently with proper embedding into the host crystal. All calculations include the fully anisotropic potentials in each cell and thus allow the reliable calculation of forces, lattice relaxations and electric field gradients. The Coulomb potential can be expressed in terms of $n(\mathbf{r})$ and therefore the force $\mathbf{F}^n$ on atom n can be derived with the use of the "ionic" Hellmann-Feynman theorem.[16] In the KKR-Green function method the electronic charge density is calculated from the imaginary part of the diagonal elements $G(\mathbf{r},\mathbf{r};E)$ of the Green function by integrating over all occupied states up to the Fermi energy E_F. Due to the analytical properties of the Green function the energy integral is replaced by a contour integral in the complex energy plane, starting at the real axis below the valence band, from there entering the complex plane and coming back to the real axis at the Fermi energy.[17] Most important is that this contour integral can be accurately calculated with only a few energy points. The hyperfine parameters of interest in the present paper are the isomer shifts (IS), the Fermi contact term of the hyperfine field (HF) and the quadrupole splitting (Δ^*). The last quantity is determined by the electric field at the probe-atom site. In a nonrelativistic treatment the isomer shift can be calculated from the charge density $n(0)$ at the nucleus

$$\mathrm{IS}=\alpha n(0), \tag{1}$$

where α is the calibration constant. The hyperfine field is given by the Fermi contact contribution in terms of the magnetization density $m(0)$ at the nucleus,

$$\Delta\mathrm{HF}=\frac{8\pi}{3}\mu_B m(0). \tag{2}$$

Finally the quadrupole splitting is calculated from

$$\Delta^*=\frac{1}{2}\frac{e|QV_{zz}|}{E_{\mathrm{source}}}\times c, \tag{3}$$

where Q is the quadrupole moment of the probe-nucleus and V_{zz} is the electric field gradient along the main (111) axis. The parameter c is the speed of light and E_{source} is the energy of the emitted γ-ray, which is 23.8 keV for Sn. The tensor of the EFG is given by the second derivatives of the Coulomb potential and can be written as[12]

$$\mathbf{V}_{\alpha\beta}=\sum_{m=-2}^{2}\tilde{V}_{2,m}(0)\partial_\alpha\partial_\beta(r^2Y_{2m}(\mathbf{r})),$$

$$\tilde{V}_{2,m}(0)=I_1+I_2,$$

$$I_1=\frac{8\pi}{5}\int_0^{R_{\mathrm{MT}}}r'^2\frac{n_{2m}(r')}{r'^3}dr',$$

$$I_2=\frac{V_{2m}(R_{\mathrm{MT}})}{R_{\mathrm{MT}}^2}-\frac{8\pi}{5}\int_0^{R_{\mathrm{MT}}}\frac{n_{2m}(r')r'^4}{R_{\mathrm{MT}}^5}dr', \tag{4}$$

where $Y_{2m}(\mathbf{r})$ are spherical harmonics, $\tilde{V}_{2,m}(r)$ are the $l=2$ components of the Coulomb potential, and R_{MT} is the muffin tin radius of the probe atom. Furthermore $n_{2m}(r)$ are the

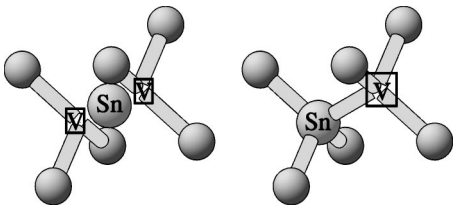

FIG. 1. The Sn-split-vacancy configuration (left) and the substitutional Sn-vacancy configuration (right).

$l=2$ components ($m=-2,\ldots,+2$) of the radial charge density. We note that just the $l=2$ components are needed for the EFGs, while the $l=1$ components enter into the forces. Consequently, the EFG vanishes for sites with cubic or tetrahedral symmetry. For the cell division of the crystal we used a generalized Voronoi construction. The impurity cell at the bond center was constructed such that it is slightly larger than the cells of the host atoms, thus avoiding to decrease the muffin tin radius of real atoms by more than 16%. To include the occupancy of the discrete gap states in the complex energy integration, we introduce two different energy contours in the complex energy plane: one, which encloses only the valence band states and comes back to the real axis slightly above the valence band maximum, and a second one, which fully encloses all gap states. Here, a group theoretical decomposition of the Green function allows us to distinguish the contributions to the charge density from different gap states. Thus, by introducing occupancy factors for the different charge density contributions, the gap states can be occupied according to their symmetry and energy.[21]

III. ELECTRONIC STRUCTURE OF Sn-VACANCY COMPLEXES

As predicted already many years ago by Watkins[1] on the basis of EPR measurements, and as has also be confirmed by *ab initio* calculations,[2,3] the stable configuration of the Sn-vacancy pair in Si consists of a Sn-atom at the bond-center position and the vacancy split in two halves on the two (empty) nearest neighbor positions. This split-vacancy configuration is shown schematically in Fig. 1 together with the "normal" substitutional complex. As we have found recently,[4] the same split-vacancy configuration occurs also upon pairing with Cd-atoms, yielding both in Si and Ge very small electric field gradients, which allow to identify this complex uniquely. In this configuration the Sn or the Cd atom are coordinated by six host atoms at the relatively large distance of 1.26 times the nearest neighbor distance (in the unrelaxed configuration).

The local density of states (LDOS) of this complex at the Sn-site in the Ge host is shown in Fig. 2 (upper panel), together with the corresponding LDOS for the Cd split-vacancy complex in Ge in Fig. 2 (lower panel). In the calculation the Fermi level is fixed at the maximum E_{val} of the valence band. The different peaks are labeled by the irreducible subspaces A_{1g}, A_{2u}, E_u, and E_g of the D_{3d} group, representing the point symmetry of the complex. Compared to the Cd complex with the *d*-level at about −9 eV, the *d*-level of

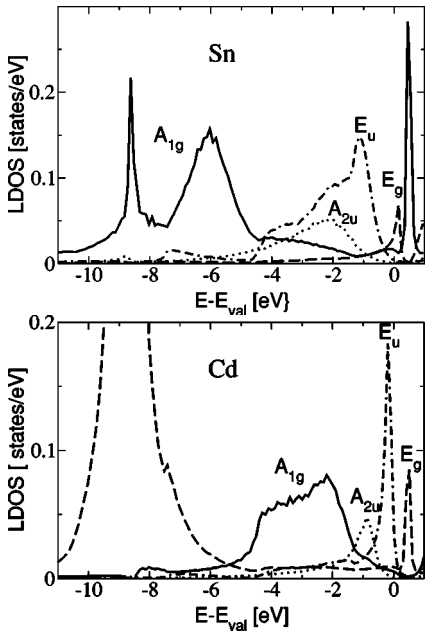

FIG. 2. LDOS projected on the irreducible subspaces of the D_{3d} group at the Sn site (above) and at the Cd site (below) for the impurity split-vacancy complex in Ge. The nearest neighbors are fixed on ideal lattice positions.

Sn is fully localized and at much lower energies. However, the overall level sequences are very similar, although the locations and the widths of the peaks are different for the two systems: the A_{1g} state lies at relative low energies, the A_{2u}, and the doubly degenerate E_u states are slightly below the Fermi level, the doubly degenerate E_g state lies in the gap. In the case of Sn, a second A_{1g} state is found at higher energies. Since the occupied A_{1g}, A_{2u}, and E_u states accommodate eight electrons, of which the six neighboring host atoms provide six (one dangling bond each), the vacancy complex with Cd (with two valence electrons) is neutral for $E_F=E_{\mathrm{val}}$ ($[\mathrm{CdV}]^0$), and the complex with Sn (with four valence electrons) is doubly positively charged ($[\mathrm{SnV}]^{2+}$). As discussed in Ref. 4, the level sequence is basically determined by the divacancy. The Cd and Sn-atoms can be considered as ionized Cd^{2+} and Sn^{4+} ions inserted in the center of the divacancy and only weakly hybridizing with the six nearest neighbors. The attractive ionic potentials shift the divacancy states to lower energies, in particular the fully symmetrical A_{1g} state, being the only state affected in the first Born approximation with respect to the potential. This effect is naturally stronger for the Sn^{4+} ion than for the Cd^{2+} ion, but the LDOS are very similar. Of course, also Cd and Sn *s* and *p* states, localized at energies above E_{val}, are hybridized into the occupied states, so that the local charge in the impurity cell is about 1 electron in the case of Cd in Ge and 2 electrons in the case of Sn in Ge. In fact, the A_{1g} state above E_F can be considered as the genuine Sn 5*s* states, which is, however, not occupied.

By occupying the E_g state in the gap, we obtain complexes with additional electron charges, i.e. $[\mathrm{SnV}]^+$, $[\mathrm{SnV}]^0,\ldots$ and analogously $[\mathrm{CdV}]^-,[\mathrm{CdV}]^{2-},\ldots$ complexes. Both the $[\mathrm{SnV}]^+$ and the $[\mathrm{SnV}]^0$ complexes are magnetic

TABLE I. The calculated hyperfine field (HF) at the Sn atom (above) and the nearest neighbor host atoms (below) for the Sn-split-vacancy in Si and Ge is shown. A comparison to the experimental values of Watkins (Ref. 1) is given.

Host	Si H_{HF} [kG]	Ge H_{HF} [kG]
$[V\|Sn\|V]^+$	139	6.00
$[V\|Sn\|V]^0$	211	14.59
Expt	241 (386 MHz)	
$[V\|Sn\|V]^+$	−39.59	−44.46
$[V\|Sn\|V]^0$	−82.96	−94.19
Expt	−91.02 (−77.00 MHz)	

with total moments of 1 and 2 μ_B, and with small local moments of 0.05 μ_B(0.008 μ_B) and 0.09 μ_B(0.02 μ_B) on the Sn site in Si (Ge). Although we have calculated only the three charge states $[SnV]^{2+}$, $[SnV]^+$, and $[SnV]^0$, calculations as well as experiments show that also the negatively charged $[SnV]^-$ and $[SnV]^{2-}$ states exist. Since for the complex $[SnV]^0$ the E_g majority state is completely filled having a moment of 2 μ_B, we expect that also the $[SnV]^-$ state is magnetic with a total moment of 1 μ_B and local moments similar to the $[SnV]^+$ complex, while the $[SnV]^{2-}$ is nonmagnetic. The existence of these five charge states arises from the fact, that the E_g state is very extended and has moreover a nodal plane at the Sn-site so that Coulomb effects are very small. This also explains the very small local moments. The situation is quite similar for Cd complexes, except that the local moments are somewhat smaller in Si, e.g. 0.02 μ_B for $[CdV]^-$. The same level sequences we expect also for other 5*sp* impurities to occur. For instance for In, the charge state should be $[InV]^+$, if E_F is fixed at E_{val}, and the $[InV]^0$, $[InV]^-$ and $[InV]^{2-}$ configurations should be magnetic. In all calculations the complexes in Si are very similar to the above results for the Ge hosts.

The calculations yield sizable relaxations of the neighboring host atoms towards the Sn atoms, which are practically radially symmetrical and increase with the charge state. For $[SnV]^{2+}$ the NN Ge atoms relax by 2.9% of the NN distance, for $[SnV]^+$ by 4.2% and $[SnV]^0$ by 5.4%. In Si the corresponding relaxations are somewhat larger: 6%, 6.2%, and 6.4%. The relaxations arise from the attraction of the neighboring electrons to the Sn^{4+} ion and increase with occupation of the E_g gap states, since these states are dangling-bond like and mostly localized at the host atoms. Therefore the neutral $[SnV]^0$ state has larger relaxations than the $[SnV]^{2+}$, which is opposite to the normal expectations.

IV. HYPERFINE PROPERTIES OF Sn-VACANCY COMPLEXES

Already Watkins[1] has measured by EPR hyperfine fields at the neighboring Si atoms adjacent to a SnV complex, which he identified as the neutral $[SnV]^0$ complex with total spin $S=1$. Table I shows the calculated hyperfine fields at the Sn atom and the six Si or Ge neighbors adjacent to the magnetic $[SnV]^+$ and $[SnV]^0$ split complexes and a comparison with the experimental values.[1,22] First we note, that the field for $[SnV]^0$ is about twice the field of $[SnV]^+$. This is a consequence of the large extent of the E_g state, representing locally a small perturbation, so that the forces increase linearly with the occupancy. Second, for $[SnV]^0$ we obtain good agreement with the experimental values. Here we note, that our calculations are non-relativistic, so that the relativistic enhancement[11] of the hyperfine field is missing, which would presumably improve the agreement. For the $[SnV]^-$ complex we expect a similar hyperfine field as for the $[SnV]^+$ complex, since the total moment is the same. We have chosen in our calculations the spin-polarization such, that the total moment has a negative sign (spin down occupation). As a consequence the local moments for all sites are negative, since the E_g state determines the magnetic properties alone. That means that $m_{loc}/H_{HF}<0$ at the Sn-site and $m_{loc}/H_{HF}>0$ at the Si nearest neighbor site. The change of sign of the hyperfine field from Si to Sn can be explained due to the different exchange interaction mechanism between the *d*-like "spin down" E_g electrons and the "spin down" and "spin up" *s*-core-electrons at the Sn-site. In the first case the interaction is attractive, leading to a smaller *s* charge density at the nucleus, whereas in the latter case the situation is opposite. In total the hyperfine field changes its sign in comparison to the Si site. In addition to the hyperfine fields we have calculated the isomer shifts and quadrupole splittings. These observables can be measured by the Mössbauer spectroscopy. Measurements using the ^{119}Sn isotope in Si and Ge were performed by Weyer *et al.*,[6,7] in 1980 which however do not agree with our calculated results. From various private discussions we conclude, that in these early experiments clustering of Sn-impurities might have occurred, leading to more complicated structures. On the other hand, our results are in good agreement with unpublished measurements of Sielemann (private communication).

TABLE II. Isomer shifts and quadrupole splitting for the Sn-vacancy complexes in Si. ($\alpha=0.2178\ a_0^3\,\mathrm{mm\,s^{-1}}$, $E_{source}=23.8$ keV, $Q=-0.124$ barn.)

System	$n(\mathbf{r}=0)$ $[a_0^{-3}]$	IS $[\mathrm{mm\,s^{-1}}]$	EFG [MHz]	Δ* $[\mathrm{mm\,s^{-1}}]$
α-Sn	87759.82	ref	0.00	0.00
subst. Sn	87758.81	−0.2200	0.00	0.00
$[V\|Sn\|V]^{2+}$	87759.71	−0.0.0257	−14.90	0.3875
$[V\|Sn\|V]^+$	87759.36	−0.1076	−10.59	0.2713
$[V\|Sn\|V]^0$	87758.99	−0.1942	−5.62	0.1473

In Table II the results for Si and in Table III the results for Ge are presented. The calibration constant α was determined by calculating $n(0)$ for several Sn-defects, for which well known isomer shifts exist. Svane *et al.*[23,24] already calculated in a relativistic treatment an α of 0.092 $a_0^3\,\mathrm{mm\,s^{-1}}$, which is in good agreement to ours with taking the Shirley factor[25] for Sn of 2.48 into account. A closer view on the isomer shifts for the Sn-split-vacancy configuration (in relation to the

TABLE III. Isomer shifts and quadrupole splitting for the Sn-vacancy complexes in Ge. (α=0.2178 a_0^3 mm s^{-1}, E_{source} =23.8 keV, Q=−0.124 barn.)

System	$n(\mathbf{r}=0)$ [a_0^{-3}]	IS [mm s^{-1}]	EFG [MHz]	Δ* [mm s^{-1}]
α-Sn	87759.82	ref	0.00	0.00
subst. Sn	87759.26	−0.1400	0.00	0.00
$[V\|Sn\|V]^{2+}$	87760.61	0.17	−12.05	0.31
$[V\|Sn\|V]^{+}$	87760.55	0.16	−8.08	0.1938
$[V\|Sn\|V]^{0}$	87760.46	0.14	−3.97	0.1027

Mössbauer line of α-Sn) shows a decreasing charge density at the nucleus with the occupation of the E_g state in the band gap. This behavior can be explained due to the screening impact of the d-like E_g-electrons at the Sn-site on the s-electrons responsible for the IS. As in the Cd case (Q_{Cd} =0.83) the Sn-EFG's are rather small, since hybridization with the neighbors is weak. It is obvious, that the EFG increases with occupying the E_g state, since p_x and p_y charges give positive contributions to the EFG at the Sn-site.

V. SUBSTITUTIONAL VERSUS SPLIT-VACANCY COMPLEXES WITH IMPURITIES

In this section we describe the results for a whole series of calculations for impurity-vacancy complexes in Si and Ge. We would like to find out for each of the 11 investigated impurities, which complex, substitutional or split-vacancy, is most stable, and to draw a border line between these two complex families as a function of the "size" of the impurities. To achieve this aim, we have performed PPW calculations for vacancy complexes with the impurities Al, Si, and P of the 3sp series, with Ga, Ge, As, and Se of the 4sp series, with Cd, In, Sn, and Sb of the 5sp series and finally with 6sp element Bi. In all cases only the neutral state has been calculated. First we discuss in detail the results for the Sn impurity in Ge.

Figure 3 shows the total energy and the force on a Sn atom, if this atom is moved adiabatically, i.e. by full relaxation of all other atoms, from the substitutional position (indicated by "relative distance 1," measured in units of the NN distance from the vacant site) to the bond center ("relative distance 0.5"). The two curves refer to the cases when the host neighbors of the complex are kept fixed at their ideal lattice positions (dashed lines), and when the six host neighbors are allowed to relax for a given Sn position (full lines). While an intermediate minimum position at about 0.75 is obtained when only the Sn atom is moved, in the case of full relaxations the Sn impurity moves without energy barrier into the stable bond center position at 0.5.

The results for all considered impurities in both Si and Ge are listed in Table IV. The second column gives the force on the impurity in the unrelaxed substitutional position, i.e., when the impurity and all neighbors are fixed at ideal lattice sites. The third column gives the energy difference between both configurations, such that for negative values the split

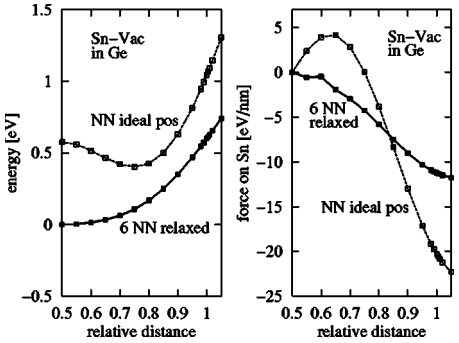

FIG. 3. Energy and force on the Sn atom for the Sn-vacancy complex in Ge as a function of the Sn position (relative coordinate in (111)-direction: 0.5 is the bond center, 1.0 the substitutional site). Presented are PPW calculations with a cut-off energy of 13.67 Ry, when the neigbors of the complex are at the ideal positions (nonrelaxed, dashed lines) and when the six NN of the complex are relaxed (full lines). On the left, the total energy is shown relative to the energy of the fully relaxed minimum configuration with Sn at the bond center site. On the right, the corresponding Hellmann-Feynman force on the Sn-atom is shown.

configuration is stable and for positive values the substitutional one. The last column gives the exact position of the impurity as measured in units of the NN distance from the vacant site.

The results show that both in Si and Ge the 5sp impurities Cd, In, Sn, and Sb as well as the 6sp impurity Bi on the substitutional site experience a strong force, which pushes them into the "free space" at the bond center, thus gaining typically an energy of 0.5–1.0 eV. Note that the energy gains are very substantial, much larger than the value 0.045 eV reported by Larsen *et al.*[2] for the Sn-vacancy complex in Si. One would intuitively classify these heavy impurities as oversized in Si and Ge. In line with this argument is the fact that the forces as well as the resulting energy gains are somewhat larger in Si than in Ge, due to the smaller lattice constant of Si. All other impurities, with the exception of Al in Si, prefer the substitutional configuration, however partly with large relaxations from the ideal position. For instance, the Ge impurity in Si is shifted by 13% of the NN distance in the direction of the vacancy and the As atom in Ge by a similar amount. Of all impurities, only the Ga impurity in both Si and Ge is shifted towards its remaining three neighbors, i.e. away from the vacancy. Therefore it is tempting to classify the Ga impurity as "undersized." The behavior of the Al impurity is most surprising. As a member of the 3sp series it should be smaller than the isoelectronic Ga impurity of the 4sp series. However the calculation seems to indicate a larger size than Ga. The force at the ideal lattice site drives the impurity in the direction of the vacancy, resulting in a split configuration for the Al-vacancy complex in Si, and in a strongly distorted substitutional configuration in Ge.

Unfortunately, we do not know any reliable rules for the "size" of impurities. Pauling[26] has given some general rules about the volume of atoms, e.g., in a tetrahedral environment. According to this, the size of impurities of the same row of the periodic table should decrease with increasing

TABLE IV. Relaxations of impurity-vacancy complexes in Si (E_{cut}=9 Ry, above) and Ge (E_{cut}= Ry, below): The first column gives the forces on the impurity atom in the substitutional positions, a negative sign means that forces are directed to towards the bond center. The second column gives the energy differences between the fully relaxed configurations with the impurity at the bond-center and at the substitutional site. The last column gives the final position of the impurity in (111) direction; 0.5 is the bond center and 1.0 is the substitutional lattice position. (∗ was obtained by the PAW method with E_{cut}=20.25 Ry.)

Impurity in Si	force [eV/nm]	$\Delta E = E_{split} - E_{subst}$ [eV]	Stable pos. in (111)
Al	−5.15	−0.15	0.50
P	−2.96	+1.27	0.95
Ga	+1.38	+0.22	1.04
Ge	−5.58	+0.30	0.87
As	−10.7	+0.82	0.90
Se	−11.5	+0.55	0.92
Cd*	−21.9*	−1.04*	0.50*
In	−19.8	−0.69	0.50
Sn	−27.0	−0.83	0.50
Sb	−33.2	−0.68	0.50
Bi	−46.8	−0.92	0.50

Impurity in Si	force [eV/nm]	$\Delta E = E_{split} - E_{subst}$ [eV]	Stable pos. in (111)
Al	−0.25	+0.03	0.82
Si	−1.16	+0.30	0.88
P	−3.01	+0.81	0.93
Ga	+3.75	+1.11	1.04
As	−11.3	+0.41	0.87
Se	−9.67	+0.35	0.91
Cd*	−17.9*	−1.01*	0.50*
In	−11.1	−0.47	0.50
Sn	−20.3	−0.60	0.50
Sb	−28.0	−0.64	0.50
Bi	−39.1	−0.86	0.50

valence, However, for the investigated cases we find just the opposite, i.e. the size increases with increasing valence, at least for the impurities of 4*sp* and 5*sp* series. For instance, As is larger than Ga, and Sb larger than In. Moreover, according to Pauling,[26] the size of isovalent impurities should increase with increasing main quantum number. As expected, our calculations confirm this second rule in general. However, deviations from both rules occur for Al: We find that Al is larger than Si and P, and in particular, is larger than the isovalent Ga impurity, which belongs to the higher 4*sp* series.

In order to shed some light on the size problem and its relation to the stability of impurity-vacancy complexes, we have calculated the lattice relaxations for the relevant isolated impurities in Si and Ge. For simplicity, we have only calculated the displacements of the nearest neighbors, by fixing all other atoms at the ideal positions. The idea behind

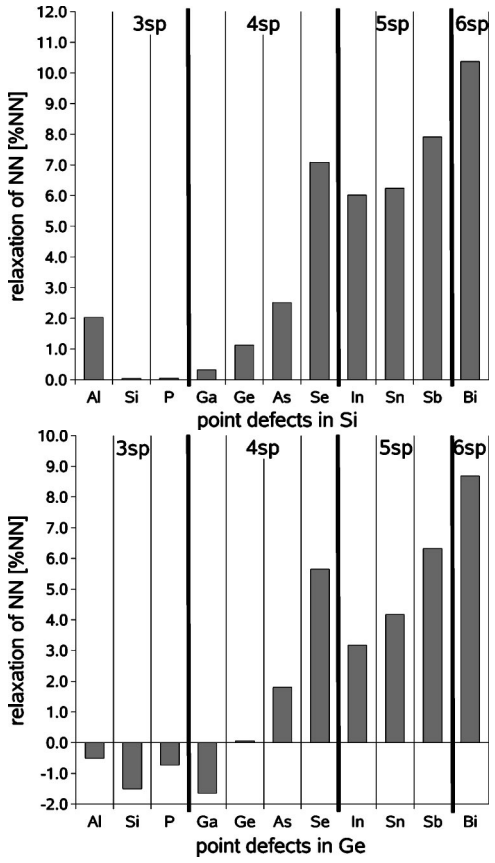

FIG. 4. Nearest-neighbor relaxations for various 3*sp*, 4*sp*, 5*sp*, and 6*sp* impurities (substitutional point defects) in Si (above) and Ge (below).

these calculations is that both problems, i.e. the NN relaxations of the impurities and the different configurations of the impurity-vacancy complexes, are directly correlated. For instance, the impurity exerts forces on the nearest neighbors, which, as a consequence, are displaced from their ideal positions. The impurity itself is not shifted, since the reaction forces of the nearest neighbors cancel each other due to the tetrahedral symmetry. However, in the case of a vacancy, one of the four neighbors is missing, so that the reaction forces of the remaining three neighbors no longer cancel each other and shift the impurity either to or away from the vacancy. In this way the pair geometry should be related to the size of the single impurities.

The calculated lattice relaxations of the nearest neighbors of the various impurities are shown in Fig. 4. They are given in percentages of the NN distance, with positive values denoting outwards relaxations. Note that in the calculations only the NN are allowed to relax (the relaxation of the higher neighbor shells is expected to increase the NN relaxations, presumable by about 30%–50%). For the 4*sp* and 5*sp* impurities we clearly find that the relaxations increase with increasing valence of the impurities. The same trend has been found in Table IV for the force on the unrelaxed impurity. Also the relaxations of the 5*sp* impurities are in general larger than the ones of the 4*sp* impurities, which is line with the fact that the forces on the unrelaxed impurity in the substitutional vacancy complex, as given in the second column

of Table IV, show the same behavior. This makes it plausible that the 5*sp* and 6*sp* impurities form a split-vacancy complex with the vacancy, while the 4*sp* impurities prefer the substitutional complex. The figure also shows the unusual behavior of the Al impurity, leading to a relatively large outward relaxation in Si and only a small inward relaxation in Ge. Thus the calculations clearly indicate that the size of Al is larger than the one of Ga, which points to an unusual behavior of Al, showing also up in the stability of the Al-split-vacancy complex in Si-bulk. Thus the NN relaxations for the isolated impurities correlate qualitatively well with the stability of the impurity-vacancy complexes. However a detailed comparison is not possible. For instance, the outward NN relaxations of the Al impurity in Si are slightly smaller than the ones of As; yet Al forms with the vacancy in Si a split complex, but As a substitutional one. Similarly, the NN relaxations of the Si impurity in Ge are inwards, but in the substitutional Si-vacancy complex Si relaxes by 12% towards the vacancy.

VI. SUMMARY

We have studied the electronic and geometrical structure of vacancy complexes with "oversized" and "normal-sized" impurities in Si and Ge. First we discuss the electronic structure of the Sn-vacancy complex. In agreement with recent *ab initio* studies for the Sn-vacancy complex in Si (Refs. 2 and 3) and in analogy to our recent studies[4] for the Cd-vacancy complex in Si and Ge, we find a split-vacancy complex as the stable configuration in both hosts with the impurity on the bond center position and the vacancy split into two "half vacancies" on the neighboring sites. The density of states of Sn and Cd are characterized by the same sequence of states and similar charge states exist. The calculated hyperfine fields of Sn and the Si neighbors are in good agreement with the measurements of Watkins.[1] However, no agreement is obtained with the available isomer shift data for Sn.[6,7]

In the second part of the paper we present a systematic study of vacancy complexes with 11 different impurities, both in Si and Ge. We find that, in both hosts, impurities of the 5*sp* and 6*sp* series form split-vacancy complexes, while impurities of the 4*sp* and 3*sp* series prefer, more or less distorted, substitutional complexes. An exception from this rule is Al, forming in Si a split complex and in Ge a strongly distorted substitutional complex. Qualitatively we explain the results in terms of the size of these impurities, such that oversized impurities can lower their energy in the "free space" available at the bond center site. To examine the "size" of these impurities, we calculated the nearest neighbor relaxations for the isolated impurities and find a good correlation between the calculated NN relaxations and the structure of the impurity-vacancy complexes.

ACKNOWLEDGMENTS

We thank R. Sielemann for helpful and motivating discussions. We gratefully acknowledge financial support by the German government, BMBF-Verbundforschung, Project No. 05KK1CJA/2.

[1] G. D. Watkins, Phys. Rev. B **12**, 4383 (1975).
[2] A. N. Larsen, J. J. Goubet, P. Mejlholm, J. S. Christensen, M. Fanciulli, H. P. Gunnlaugsson, G. Weyer, J. W. Petersen, A. Resende, M. Kaukonen, R. Jones, S. Öberg, P. R. Briddon, B. G. Svensson, J. L. Lindström, and S. Dannefaer, Phys. Rev. B **62**, 4535 (2000).
[3] M. Kaukonen, R. Jones, S. Öberg, and P. R. Briddon, Phys. Rev. B **64**, 245213 (2001).
[4] H. Höhler, N. Atodiresei, K. Schroeder, R. Zeller, and P. H. Dederichs, Phys. Rev. B **70**, 155313 (2004).
[5] Paola Alippi, Antonino LaMagna, Silvia Scalese, and Vittorio Privitera, Phys. Rev. B **69**, 085213 (2004).
[6] G. Weyer, A. Nylandsted Larsen, N. E. Holm, and H. L. Nielsen, Phys. Rev. B **21**, 4939 (1980).
[7] G. Weyer, S. Damgaard, J. W. Petersen, and J. Heinemeier, Phys. Lett. **76A**, 321 (1980).
[8] S. H. Vosko, L. Wilk, and M. Nusair, Can. J. Phys. **58**, 1200 (1980).
[9] P. J. Braspenning, R. Zeller, A. Lodder, and P. H. Dederichs, Phys. Rev. B **29**, 703 (1984).
[10] N. Papanikolaou, R. Zeller, and P. H. Dederichs, J. Phys.: Condens. Matter **14**, 2799 (2002).
[11] H. Akai, M. Akai, S. Blügel, B. Drittler, H. Ebert, K. Terakura, R. Zeller, and P. H. Dederichs, Prog. Theor. Phys. Suppl. **101**, 11 (1990).
[12] P. Blaha, K. Schwarz, and P. H. Dederichs, Phys. Rev. B **37**, 2792 (1988); **38**, 9368 (1988).
[13] L. Kleinman, D. M. Bylander, Phys. Rev. Lett. **48**, 1425 (1982).
[14] R. Berger, S. Blügel, A. Antons, Wi. Kromen, and K. Schroeder, in *Proceedings of the NIC-Workshop "Molecular Dynamics on parallel Computers"*, Jülich, 08.-10. February 1999 (World Scientific, Singapore, 2000), p. 185–198.
[15] J. D. Pack and H. J. Monkhorst, Phys. Rev. B **16**, 1748 (1977).
[16] N. Papanikolaou, R. Zeller, P. H. Dederichs, and N. Stefanou, Phys. Rev. B **55**, 4157 (1997).
[17] R. Zeller, J. Deutz, and P. H. Dederichs, Solid State Commun. **44**, 993 (1982).
[18] M. Asato, A. Settels, T. Hoshino, T. Asada, S. Blügel, R. Zeller, and P. H. Dederichs, Phys. Rev. B **60**, 5202 (1999).
[19] R. Zeller, P. H. Dederichs, B. Újfalussy, L. Szunyogh, and P. Weinberger, Phys. Rev. B **52**, 8807 (1995).
[20] R. Zeller, Phys. Rev. B **55**, 9400 (1997).
[21] A. Settels, Ph.D. thesis, RWTH Aachen, 1999.
[22] M. Fanciulli and J. R. Byberg, Phys. Rev. B **61**, 2657 (2000).
[23] A. Svane, J. Phys. C **21**, 5369 (1988).
[24] A. Svane, N. E. Christensen, C. O. Rodriguez, and M. Methfessel, Phys. Rev. B **55**, 12 572 (1997).
[25] D. A. Shirley, Rev. Mod. Phys. **36**, 339 (1964).
[26] L. Pauling, *The Nature of the Chemical Bond and the Structure of Molecules and Crystals* (Cornell University Press, Ithaca, 1960).